CFAP70 mutations lead to male infertility due to severe astheno-teratozoospermia.

Julie Beurois, Guillaume Martinez, Caroline Cazin, Zine-Eddine Kherraf, Amir Amiri-Yekta, Nicolas Thierry-Mieg, Marie Bidart, Graciane Petre, Véronique Satre, Sophie Brouillet, et al.

CFAP70 mutations lead to male infertility due to severe astheno-teratozoospermia.

Julie Beurois[1,£], Guillaume Martinez[1,2,£], Caroline Cazin[1,£], Zine-Eddine Kherraf[1,3], Amir Amiri-Yekta[4], Nicolas Thierry-Mieg[5], Marie Bidart[6], Graciane Petre[6], Véronique Satre[1,2], Sophie Brouillet[7], Aminata Touré[8,9,10], Christophe Arnoult[1], Pierre F. Ray[1,3,$] and Charles Coutton[1,2,$,*]

[1] Univ. Grenoble Alpes, INSERM U1209, CNRS UMR 5309, Institute for Advanced Biosciences, Team Genetics Epigenetics and Therapies of Infertility, 38000 Grenoble, France.

[2] CHU Grenoble Alpes, UM de Génétique Chromosomique, Grenoble, France.

[3] CHU de Grenoble, UM GI-DPI, Grenoble, F-38000, France

[4] Department of Genetics, Reproductive Biomedicine Research Center, Royan Institute for Reproductive Biomedicine, ACECR, Tehran, Iran

[5] Univ. Grenoble Alpes / CNRS, TIMC-IMAG, F-38000 Grenoble, France

[6] Univ. Grenoble Alpes / INSERM U1205, UFR Chimie Biologie, Grenoble, France.

[7] Université Grenoble-Alpes, Laboratoire d'AMP-CECOS, CHU Grenoble-Alpes, U1036 INSERM-UGA-CEA-CNRS, 38000 Grenoble, France

[8] INSERM U1016, Institut Cochin, Paris 75014, France.

[9] Centre National de la Recherche Scientifique UMR8104, Paris 75014, France.

[10] Faculté de Médecine, Université Paris Descartes, Sorbonne Paris Cité, Paris 75014, France.

[£] The authors should be regarded as first authors respectively.

[$] The authors should be regarded as last authors respectively.

* Corresponding author: Charles COUTTON, Laboratoire de Génétique Chromosomique, Hôpital Couple Enfant, CHU Grenoble Alpes, 38043 Grenoble cedex 9, France. Tel: +33-4-76-76-54-82; E-mail: CCoutton@chu-grenoble.fr

Abstract

The use of high-throughput sequencing techniques allowed to identify numerous mutations in genes responsible for severe astheno-teratozoospermia due to multiple morphological abnormalities of the sperm flagella (MMAF). However, more than half of the analyzed cases remains unresolved suggesting that many yet uncharacterized gene defects account for this phenotype. Based on whole-exome sequencing data from a large cohort of 167 MMAF-affected subjects, we identified two unrelated affected individuals carrying a homozygous deleterious mutation in *CFAP70*, a gene not previously linked to the MMAF phenotype. One patient had a homozygous splice variant c.1723-1G>T, altering a consensus splice acceptor site of *CFAP70* exon 16 and one had a likely deleterious missense variant in exon 3 (p.Phe60Ile). *CFAP70* gene encodes a regulator protein of the outer dynein arms (ODA) strongly expressed in human testis. In the sperm cells from the patient carrying the splice variant, immunofluorescence experiments (IF) confirmed the absence of the protein in the sperm flagellum. Moreover, IF analysis showed the absence of markers for the outer dynein arms and the central-pair complex of the axoneme.. Interestingly, whereas CFAP70 staining was present in sperm cells from patients with mutations in the three other MMAF-related genes *ARMC2, FSIP2* and *CFAP43,* we observed an absence of staining in sperm cells from patients mutated in the *WDR66* gene, suggesting a possible interaction between these two axonemal components. In conclusion, this work provides the first evidence that loss of CFAP70 function causes MMAF, and that ODA-related proteins may be crucial for the assembly and/or stability of the flagellum axoneme in addition to its motility.

Key words: Male infertility, genetics, MMAF, CFAP70, outer dynein arm, gene mutation, flagellum, whole-exome sequencing.

Introduction

The past decade has been marked by the emergence of the next generation sequencing (NGS), a fast evolving technology which allowed important advances in human genetics. This technical revolution has proved to be a highly powerful research and diagnostic tool in male infertility and permitted to take a major step forward for the identification of the genetic cause of male infertility (Krausz and Riera-Escamilla, 2018). In particular, NGS has contributed massively to decipher the genetic causes involved in multiple morphological abnormalities of the flagella (MMAF phenotype) which is a subgroup of astheno-teratozoospermia characterized by the presence in the ejaculate of immotile spermatozoa with several flagellar defects including short, coiled, absent and flagella of irregular caliber (Ray *et al.*, 2017). To date, mutations in fourteen genes have been found to be associated with MMAF (*AK7, AKAP3, AKAP4, ARMC2, CEP135, CFAP43*, *CFAP44*, *CFAP65, CFAP69*, *DNAH1, FSIP2, QRICH2, TTC21A* and *WDR66*) (Supplementary Fig. S1) (Baccetti *et al.*, 2005; Ben Khelifa *et al.*, 2014; Sha *et al.*, 2017a; Tang *et al.*, 2017; Auguste *et al.*, 2018; Coutton *et al.*, 2018; Dong *et al.*, 2018; Kherraf *et al.*, 2018; Lorès *et al.*, 2018; Martinez *et al.*, 2018; Coutton *et al.*, 2019; Liu *et al.*, 2019; Shen *et al.*, 2019). However, despite these plethoric findings, the etiology of MMAF remains unknown in more than 50% of the cases and the discovery of the remaining genes is a now a major challenge (Coutton *et al.*, 2019).

Using different animal models and in particular flagellated protists such as Chlamydomonas or Trypanosoma, at least five of these known MMAF-related genes (*DNAH1*, *CFAP43*, *CFAP44*, *WDR66* and *CEP135)* have been already reported to encode different components of the axoneme, a central multi-protein complex which is highly conserved throughout evolution and shared by both the sperm flagellum and other motile cilia (Inaba, 2007; Satir and Christensen, 2008). Briefly, the axoneme consists of 9 outer doublet microtubules (DMTs) surrounding 2 central singlets (9+2 structure) known as the central pair

complex (CPC). DMTs carry several components that drive and regulate ciliary or flagellar motility including axonemal dynein motors subdivided into inner (IDA) and outer arms (ODA), radial spokes, nexin links and many other (Satir and Christensen, 2008). DNAH1 is located in the inner dynein arm which drives axoneme bending and ciliary or flagellar motility (Ben Khelifa *et al.*, 2014), CFAP43 and CFAP44 seem to be related to the the tether and tether head (T/TH) complex, which connects dynein motor domains to DMTs (Fu *et al.*, 2018; Urbanska *et al.*, 2018), WDR66 is a component of the spoke-associated complex (CSC) which mediates regulatory signals between the radial spokes and dynein arms (Urbanska *et al.*, 2015) and CEP135 is located in the centrosomal complex (Ohta *et al.*, 2002). In this work, we analyzed genetic data obtained by whole-exome sequencing (WES) from a large cohort of 167 MMAF patients, and identified two patients carrying a homozygous deleterious mutation in the *CFAP70* gene, which encodes an axonemal protein that is localized at the base of the outer dynein arm and regulates ciliary motility (Shamoto *et al.,* 2018). Therefore, this work shows for the first time the involvement of an ODA-linked protein to the MMAF phenotype and confirmed that the ODA complex, in addition to its motility function, plays an important role in the assembly and/or the stability of the flagellum axoneme.

Case report

WES was performed on a large cohort of 167 MMAF patients as previously described (Coutton *et al.*, 2019). All individuals presented with a typical MMAF phenotype characterized by severe asthenozoospermia (total sperm motility below 10%) with at least three of the following flagellar abnormalities present in >5% of the spermatozoa: short, absent, coiled, bent or irregular flagella (for details see Coutton *et al.,* 2019). Sperm analysis was carried out in the clinical laboratories during routine biological examination of the patient according to World Health Organization (WHO) guidelines (Wang *et al.*, 2014). The

morphology of the sperm cells from the *CFAP70* mutated patients was assessed with Papanicolaou staining (Fig. 1A). Detailed semen parameters of the two mutated patients are presented in Table I. All individuals have a normal somatic karyotype (46,XY) with normal bilateral testicular size, normal hormone levels and secondary sexual characteristics. Informed consent was obtained from all the subjects participating in the study according to local protocols and the principles of the Declaration of Helsinki. The study was approved by local ethics committees, and samples were then stored in the CRB Germethèque (certification under ISO-9001 and NF-S 96-900) following a standardized procedure or were part of the Fertithèque collection declared to the French Ministry of health (DC-2015-2580) and the French Data Protection Authority (DR-2016-392).

Bioinformatics analysis was performed according to our previously described protocol (Coutton *et al.*, 2019). Data analysis of the whole cohort of 167 MMAF individuals permitted to identify 54 individuals (32.3 %) with harmful mutations in known MMAF-related genes (Coutton *et al.*, 2019). In addition, we identified here two patients (CFAP70_1 and CFAP70_2) with a homozygous deleterious variant in *CFAP70*, a gene not previously associated with any pathology, accounting for 1.2% of our cohort. The *CFAP70* mutations were subsequently validated by Sanger sequencing (Fig. 1B). PCR primers are listed in Supplementary Table S1 and a detailed protocol can be found in Coutton *et al.*, (2019). The first variant identified in the patient CFAP70_1 is a splice variant c.1723-1G>T, altering a consensus splice acceptor site of *CFAP70* exon 16 (Fig. 1C). The second variant identified in individual CFAP70_2 is a missense variation c.178T>A (p.Phe60Ile) located in exon 3 (Fig. 1C). Both variants were absent from gnomAD, the largest control sequence database regrouping sequence data from over 120 000 individuals. No mRNA analysis or immunostaining could be performed on sperm cells from CFAP70_2 due to the lack of biological samples. However, using prediction software for non-synonymous SNPs we found that this missense change is predicted to be

deleterious by SIFT (score of 0) and probably damaging by PolyPhen (score of 0.996). Moreover, the concerned amino acid (Phe60) was found conserved in *CFAP70* orthologs (Fig. 1D). For these two patients, no other candidate variants reported to be associated with cilia, flagella or male fertility were found.

CFAP70 (NM_145170.3, formerly reported as *TTC18*) is located on chromosome 10 and contains 27 exons encoding a predicted 1121-amino acid protein (Q5T0N1). *CFAP70* is predominantly expressed in the testis according to data from GTEx (GTEx Consortium, 2015) and described to be associated with cilia and flagella (Shamoto *et al.*, 2018). RT-qPCR experiments performed with a panel of ten human tissues including other ciliated tissues such as trachea confirmed these results showing that *CFAP70* transcripts are most highly expressed in the testis compared to all the other tested tissues (Supplementary Fig. S2). Primers sequences and RT-qPCR conditions are indicated in Supplementary Table S2 and in Coutton *et al.*, (2019). According to the Uniprot server, CFAP70 contains 8 tetratricopeptide repeats (TPR-repeat), which are known to form scaffolds which mediate protein-protein interactions (The UniProt Consortium, 2017) (Fig. 1C).

We performed immunofluorescence (IF) assays on sperm cells from fertile control, patient CFAP70_1 carrying the splice variant c.1723-1G>T and other MMAF patients mutated in other genes. For each MMAF patients studied, 200 sperm cells were analyzed by two different experienced operators and the IF staining intensity and pattern were compared to a fertile control. CFAP70 immunostaining in sperm cells from control was present all along of the flagellum, with a marked signal at the base of the flagellum. In the CFAP70_1 patient the CFAP70 staining was totally absent in all analyzed spermatozoa (Fig. 2) confirming the deleterious effect of this mutation. In order to determine if the loss of CFAP70 was specifically linked to the *CFAP70* mutation and was not a hallmark of the MMAF phenotype, secondary to structural defects, we performed IF assays on sperm cells from five other

MMAF patients including four patients previously identified with a mutation in *ARMC2*, *FSIP2, CFAP43*, *WDR66* and one with no genetic cause identified (Fig. 2). Genotype information of the four additional MMAF patients mutated in *ARMC2*, *FSIP2*, *CFAP43* and *WDR66* are indicated in Supplementary Table S3. In all but the *WDR66* mutated patient, CFAP70 immunostaining was comparable with what was observed on fertile controls (Fig. 2), indicating that CFAP70 expression and localization was not altered in the sperm from MMAF patients with mutations in these genes. Interestingly, CFAP70 staining was mostly absent in the *WDR66*-mutated patient irrespective of the sperm morphology (Supplementary Fig. S3) suggesting a possible link, direct or indirect, between these two axonemal components in the sperm flagellum (Fig. 2).

To further characterize the molecular defects induced by *CFAP70* mutations in human sperm, we used an indirect approach studying by IF the presence and localization of some proteins belonging to different sub-structures of the axoneme. The presence of the only two following proteins was investigated: SPAG6 as a marker of the CPC and DNAI2 as markers of outer dynein arm (ODA). We observed that in sperm from individual CFAP70_1, staining of SPAG6, an axoneme central pair complex protein (Sapiro *et al.*, 2000), was totally absent from the flagellum (Fig. 3) showing defects in the CPC structure (Fig. 3). This finding is in concordance with previous results showing that the absence of CPC is a frequent characteristic of MMAF spermatozoa (Coutton *et al.*, 2015). Similarly, the staining of DNAI2 was totally absent or dramatically reduced in most of the analyzed sperm irrespective of the sperm morphology (Fig. 4). This result is consistent with the function of CFAP70 as a regulatory component of the ODA in motile cilia and flagella (Shamoto *et al.*, 2018). To formally conclude, all the potential ultrastructural defects observed using IF should be further confirmed by Transmission Electron Microscopy (TEM). However, TEM could not be performed in this present work due to a very low amount of sperm cells available. As well,

due to limited sample availability, IF analyses could not be repeated on sperm from the other *CFAP70_2* mutated patient.

Discussion

In this present work, we identified two infertile patients with typical MMAF phenotype carrying deleterious homozygous mutations in the *CFAP70* gene. The first patient harbors a deleterious splicing mutation leading to the absence of the protein in the sperm flagellum (Fig. 2). The second patient has a missense mutation at position Phe60 predicted to be deleterious using mutation-prediction software. However, bioinformatics predictions are not sufficient to conclude to the pathogenicity of this mutation and additional supporting functional work (e.g. mRNA or protein studies, IF experiments or CRISPR/Cas9-targeted mutagenesis in different animal models) could be useful to reinforce this assumption. Mutations in *CFAP70* appeared as the best candidates to explain the MMAF phenotype observed in these two patients based on robust evidence in the literature supporting its critical function for cilia/flagella formation and function. First, transcriptomic studies showed that *Cfap70* was strongly upregulated in differentiating mouse tracheal epithelial cells (Xu *et al.*, 2015). Furthermore, inactivation of *ttc18*, the orthologue of the human *CFAP70* in zebrafish, led to a significant reduced cilia length and number in the Kupffer's vesicle (Dam *et al.*, 2017). Moreover, extensive work on Chlamydomonas FAP70 demonstrated that the protein is a regulator of the ODA (Shamoto *et al.*, 2018). Importantly, the authors demonstrated that FAP70 is not formally a component of the ODA complex but seems to be involved in the coordination of the ODA activity in response to changes in the surrounding mechanical and/or chemical conditions to produce proper ciliary motility (Shamoto *et al.*, 2018). In this work, IF experiments showed ODA defects in sperm cells from CFAP70_1 patient (Fig. 4). Moreover, previous studies demonstrated that the ODA were not disorganized in sperm flagellum from

MMAF patients mutated in other axonemal genes suggesting that ODA defects may be specifically linked to *CFAP70* mutations. In Chlamydomonas, the lack of FAP70 did not affect the ODA ultrastructure (Shamoto *et al.*, 2018), in contrast to what was observed in the sperm cells from our patient (Fig. 4). However, such discrepancy between human and flagellate flagella was already found for two other genes involved in MMAF (*CFAP43* and *CFAP44*) (Coutton *et al.*, 2018). These IF results should nevertheless be confirmed by TEM analysis in sperm cells from CFAP70 mutated patients to allow reliable and definitive conclusions.*CFAP70* encodes a TPR protein composed of 8 TPR-repeats located at the C-terminal domain. TPR domains are known to mediate protein–protein interactions and it has been proposed that FAP70 localizes at the base of ODA through the N-terminal end of the protein and the C-terminal region may define the binding partner that regulates ODA function (Shamoto *et al.*, 2018). CFAP70's partners are still unknown but Shamoto et al. (2018) suggested that CFAP70 could interact with various ciliary regulatory proteins such as protein phosphatases (Elam *et al.*, 2011) and calcium-binding proteins (Mizuno *et al.*, 2012). Interestingly, we showed in the present study that the CFAP70 staining is absent in a patient with mutation in the *WDR66* gene. *WDR66* is a MMAF-related gene previously reported which encodes an axonemal protein containing a calcium-regulating EF-hand domain in its C-terminal end (Auguste *et al.,* 2018; Kherraf *et al.,* 2018). Interestingly, the WDR66 patient included in this present work harbored the recurrent terminal deletion previously described to remove the C-terminal domain of the protein (Kherraf *et al.,* 2018). Therefore, this observation may suggest an additional role of the C-ter domain of CFAP251 in the recruitment and assembly of other component of the flagellum as CFAP70 may be. Moreover, WDR66 has been described to localize to the calmodulin- and spoke-associated (CSC) complex at the base of radial spoke 3 in *Tetrahymena* and *Chlamydomonas* (Urbanska *et al.,* 2015). Interestingly, the CSC is involved in the modulation of dynein activity and

therefore in the regulation of flagellar motility (Heuser *et al.*, 2012). These findings support the fact that WDR66 is a potential partner of CFAP70 and may work in synergy to modulate inner and outer dynein activity. However, further investigations (such as co-immunoprecipitation (co-IP) experiments) are necessary to clarify this hypothesis and will permit to elucidate the mechanisms by which CFAP70 regulates ODA function and flagellum and cilia length in mammals.

Last, it has been demonstrated that *Cfap70* inactivation in mouse ependymal cells led to shortened cilia in addition to motility defects (Shamoto *et al.,* 2018). This observation echoes the sperm phenotype observed in our two MMAF patients presenting sperm with short and immotile flagella. Moreover, this supports our findings that CFAP70 may be involved in axoneme biogenesis or stability beyond its function in ODA regulation.

As observed for the other MMAF individuals of the cohort (Coutton *et al.*, 2019), analysis of sperm morphology from patients CFAP70_$_{1\text{-}2}$ showed a high proportion of spermatozoa with abnormal flagella (Fig. 1, Table I). Interestingly, we also found low sperm concentrations in the ejaculates (oligozoospermia) as was observed for patients mutated in *CFAP69* (Dong *et al.*, 2018). However, the two CFAP70 patients presented a different pattern of morphological defects of the sperm flagellum with only short flagella for the patient 1 while a mosaic of defects (short, absent or irregular caliber) was observed in patient 2. In addition, patient CFAP70_$_1$ with the most severe variant presents spermatozoa with 0% motility in contrast with the patient with the missense variant (p.Phe60Ile), who presents a milder phenotype with 13% motility (Table I). This could suggest that the Phe60Ile mutated protein may preserve a residual activity as it was reported for other missense mutations in other MMAF-related genes (Ben Khelifa *et al.*, 2014; Amiri-Yekta *et al.*, 2016). Moreover, this may reinforce the hypothesis of a possible phenotype continuum depending on the severity of mutations in MMAF genes as showed for *DNAH1* (Ben Khelifa *et al*., 2014).

Concerning the prognosis of ICSI using sperm cells from *CFAP70*-mutated subjects, only ICSI outcomes for the patient CFAP70_1 were available, and one clinical pregnancy with one live birth after two cycles was reported. This positive outcome is consistent with previous studies demonstrating that MMAF affected individuals have a good prognosis following ICSI (Coutton *et al.*, 2015; Wambergue *et al.*, 2016; Sha *et al.*, 2017b).

Last, we know that *CFAP70* is expressed in different ciliated tissues such as trachea or ependymal epithelium. However, the two patients with CFAP70 mutations presented only with primary infertility without any other clinical features, thus excluding a phenotype of Primary Cilia Dyskinesia (PCD) as was observed for all genes associated with a MMAF phenotype. These recurrent observations confirm once again that flagellum biogenesis requires some proteins and pathways that are at least partly different from those necessary for cilia biogenesis. Interestingly, we observed that many of these MMAF-related genes encode proteins which are linked directly or indirectly with the protein complex close to the radial spoke 3 (RS3) (DNAH1, WDR66, CFAP43, CFAP44 and now CFAP70) suggesting that the RS3 biogenesis and function may be one of the major differences between cilia and sperm flagella.

Supplementary data

Supplementary data are available at Human Reproduction online.

Acknowledgments

We thank all patients and control individuals for their participation.

Authors' roles

J.B., C.C., G.M., P.F.R., C.A., S.B., and A.T. analyzed the data and wrote the manuscript; Z-E.K., N.T-M., P.F.R. and C.C. performed and analyzed genetic data; J.B., C.C. and G.M. performed IF experiments. G.P., M.B. performed RT-qPCR experiments; A.A-Y., V.S. provided clinical samples and data; C.C., P.F.R., C.A. and G.M. designed the study, supervised all molecular laboratory work, had full access to all of the data in the study and takes responsibility for the integrity of the data and its accuracy. All authors contributed to the report.

Funding

This work was supported by following grants: the 'MAS-Flagella' project financed by the French ANR and the DGOS for the program PRTS 2014 and the 'Whole genome sequencing of patients with Flagellar Growth Defects (FGD)' project financed by the Fondation Maladies Rares for the program Séquençage à haut débit 2012.

Conflict of interest

The authors have declared that no conflict of interest exists.

Figure Legends

Figure 1 Morphology of normal and CFAP70 mutant spermatozoa, and the mutations identified in the *CFAP70* gene. (**A**) Light microscopy analysis of spermatozoa from fertile control and individual CFAP70_1. All spermatozoa from the patient have shorter flagella than controls. Additional features of MMAF spermatozoa such as thick and coiled flagella are also observed. Scale bars 10 µm. (**B**) Electropherograms of Sanger sequencing showing the two *CFAP70* variants identified in the MMAF cohort. The substituted nucleotides are highlighted in red. (**C**) Location of *CFAP70* mutations in the intron-exon structure and in the protein representation. Blue square stands for tetratricopeptide repeats (TPR) as predicted by InterPro server (https://www.ebi.ac.uk/interpro/). Mutations are annotated in accordance to the HGVS's recommendations. (**D**) Amino-acid sequences alignment of CFAP70 in different vertebrate species showing the conservation of the amino-acid (Phe, F) in position 60 (highlighted in red) as well as the surrounded amino-acids.

Figure 2 CFAP70 immunostaining in human spermatozoa from control and MMAF patients. Sperm cells from a fertile control, the patient CFAP70_1, four other MMAF patients mutated in *ARMC2*, *FSIP2, CFAP43*, *WDR66* and one MMAF patient with unknown genetic cause were stained with anti-CFAP70 (HPA037582, Sigma-Aldrich, rabbit, 1:100, green) and anti-acetylated tubulin (32-2500, ThermoFisher, mouse, 1: 1000, red) antibodies. DNA was counterstained with DAPI showing sperm nuclear DNA (blue). The CFAP70 immunostaining (green) uniformly decorates the full-length flagellum from the fertile control, the three patients mutated in *ARMC2*, *FSIP2, CFAP43* and the MMAF patient with unknown genetic cause. Conversely, CFAP70 staining is absent in sperm from the CFAP70$_{_1}$ patient mutated in

CFAP70 and the patient mutated in *WDR66*. Mutations are specified for each patient. Scale bars 10 μm.

Figure 3 Outer dynein arms are affected by *CFAP70* mutations.

Sperm cells from a fertile control and the patient CFAP70_1 were stained with anti-SPAG6 (HPA038440, Sigma-Aldrich, rabbit, 1:500, green), a protein located in the CP complex, and anti-acetylated tubulin (32-2500, ThermoFisher, mouse, 1:1000, red) antibodies. DNA was counterstained with DAPI. SPAG6 staining is mostly absent in sperm from the patient mutated in *WDR66* irrespective of the sperm morphology (short, long, coiled or disorganized). The histogram showing the percentage of analyzed spermatozoa with or without the SPAG6 staining according to their morphology are presented (number of sperm cells analyzed = 200). Scale bars 10μm.

Figure 4 The central pair complex are affected by *CFAP70* mutations. Sperm cells from a fertile control and the patient CFAP70_1 were stained with anti-DNAI2 (H00064446-M01, Abnova, mouse, 1:400, red), a protein located in the outer dynein arm, and anti-acetylated tubulin (PA5-19489, ThermoFisher, rabbit, 1:500, green) antibodies. DNA was counterstained with DAPI. The DNAI2 immunostaining is moslty absent or dramaticcaly reduced in sperm from the patient CFAP70_1 compared to the fertile control and irrespective of the sperm morphology (short, long, coiled or disorganized). The histogram showing the percentage of analyzed spermatozoa with or without the DNAI2 staining according to their morphology are presented (number of sperm cells analyzed = 200). Scale bars 10μm

Tables

Table I Detailed semen parameters for the two MMAF individuals harboring a *CFAP70* mutation.

***CFAP70* mutated patients**		**Semen parameters**																
Patients	*CFAP70* mutations	Sperm volume (ml)	Sperm conc.(10^6/ml)	Total motility 1 h	Vitality	Normal spermatozoa	Absent flagella	Short Flagella	Coiled Flagella	Bent Flagella	Flagella of irregular caliber	Tapered head	Thin head	Micro-cephalic	Macro-cephalic	Multiple heads	Abnormal base	Abnormal acrosomal region
CFAP70_1	c.1723-1G>T	2.5	2	0	75	0	0	90	0	0	0	10	0	1	0	0	0	0
CFAP70_2	c.178T>A	3	6.9	13	72	0	28	24	10	0	58	10	4	0	2	0	54	80
Reference limits[a]		1.5 (1.4-1.7)	15 (12-16)	40 (38-42)	58 (55-63)	23 (20-26)	5 (4-6)	1 (0-2)	17 (15-19)	13 (11-15)	2 (1-3)	3 (2-4)	14 (12-16)	7 (5-9)	1 (0-2)	2 (1-3)	42 (39-45)	60 (57-63)

Values are percentages unless specified otherwise
[a]Reference limits (5th centiles and their 95% confidence intervals) according to the World Health Organization

Supplementary data

Supplementary figures

Figure S1 Structure of mature mammalian sperm cells and localization of proteins whose functional absence leads to MMAF phenotype in human.

Schematic cross sections through a representative segment of the intermediate piece (IP), principal piece (PP) and terminal piece (TP) are shown. The axoneme is enlarged and the offset shows: the 9 outer microtubule doublets of the axoneme with associated inner dynein arms, outer dynein arms, radial spokes, nexin-dynein regulator complex, nexin links and the central pair of microtubule doublets. Proteins encoded by the MMAF-related genes identified by our team (red) and by other teams (green) in human are reported. Proteins with a "?" indicated a possible localization but not yet formally demonstrated. CFAP65 localization is totally unknown and not indicated.

Figure S2 Relative mRNA Expression of human *CFAP70* transcripts.

CFAP70 mRNA levels in a panel of 10 human normal tissues purchased from Life Technologies®. Results are presented as the mean of triplicates (ratio target gene/RPL6) ± Standard Deviation (SD). RT-qPCR data were normalized using the reference gene RPL6 with the -ΔΔCt method. Heart expression is arbitrary set to 1. *CFAP70* has the strongest expression in testis compared to other organs. Unpaired t-test, ***P< 0.001.

Figure S3 CFAP70 immunostaining in human spermatozoa from the *WDR66* mutated patient according to various flagellum defects.

Sperm cells from a fertile control and one patient harboring the homozygous c.3007_3337del mutation in *WDR66* were stained with anti-CFAP70 (HPA037582, Sigma-Aldrich, rabbit, 1:100, green) and anti-acetylated tubulin (32-2500, ThermoFisher, mouse, 1: 1000, red) antibodies. DNA was counterstained with DAPI showing sperm nuclear DNA (blue). CFAP70 staining is mostly absent in sperm from the patient mutated in *WDR66* irrespective of the sperm morphology (short, long, coiled or disorganized). The histogram showing the percentage of analyzed spermatozoa with or without the CFAP70 staining according to their morphology are presented (number of sperm cells analyzed = 200). Scale bars 10µm.

Supplementary tables

Table S1 Primer sequences used for Sanger sequencing verification of *CFAP70* variations and respective melting temperatures (Tm).

Primer names	Primer sequences (5'-3')	Tm
CFAP70-3F	GACTCCAACATAACAGCACTTCA	59°C
CFAP70-3R	GGAAGAAGGCAATCGGGACA	
CFAP70-16F	GCTGATAGTCTACCACCCACC	59°C
CFAP70-16R	TTGTGTTTTCAGTGCCTAGCA	

Table S2 Primers used for RT-qPCR of *CFAP70* in human.

Primer names	Primer sequences (5'-3')	Tm
CFAP70_qPCR_8F	TGGGACTTGGAAAGTCGCTG	58°C
CFAP70_qPCR_9R	GCAATCGGCAATTCGCTTCT	
RPL6_qPCR_F	TCCATTCGTCAGAGCAAACA	56°C
RPL6_qPCR_R	TACGGAGCAGCGCAAGAT	

Table S3. Genotype information of the four additional MMAF patients mutated in *ARMC2*, *FSIP2, CFAP43* and *WDR66* included in this study.

Gene	Variant coordinates	Transcript	cDNA Variation	Amino acid variation	Allelic status	References
CFAP43	chr10:105912486	ENST00000357060	c.3541-2A>C	p.Ser1181Lysfs*4	Homozygous	Coutton *et al.,* 2018
WDR66	chr12:122355768_122441833	ENST00000288912.8	c.[3007_3337del]	p.Ile1003Lysfs26	Homozygous	Kherraf *et al.,* 2018
FSIP2	chr2:185805693	ENST00000424728	c.[16389_16392delAATA]	p.Glu5463GlufsTer7	Homozygous	Martinez *et al.,* 2018
ARMC2	chr6:108904406	ENST00000392644.8	c.1023+1G>A	splice_donor_variant	Homozygous	Coutton *et al.,* 2019

REFERENCES

Amiri-Yekta A, Coutton C, Kherraf Z-E, Karaouzène T, Le Tanno P, Sanati MH, Sabbaghian M, Almadani N, Sadighi Gilani MA, Hosseini SH, *et al.* Whole-exome sequencing of familial cases of multiple morphological abnormalities of the sperm flagella (MMAF) reveals new DNAH1 mutations. *Hum Reprod Oxf Engl* 2016;**31**:2872–2880.

Auguste Y, Delague V, Desvignes J-P, Longepied G, Gnisci A, Besnier P, Levy N, Beroud C, Megarbane A, Metzler-Guillemain C, *et al.* Loss of Calmodulin- and Radial-Spoke-Associated Complex Protein CFAP251 Leads to Immotile Spermatozoa Lacking Mitochondria and Infertility in Men. *Am J Hum Genet* 2018;**103**:413–420.

Baccetti B, Collodel G, Estenoz M, Manca D, Moretti E, Piomboni P. Gene deletions in an infertile man with sperm fibrous sheath dysplasia. *Hum Reprod Oxf Engl* 2005;**20**:2790–2794.

Ben Khelifa M, Coutton C, Zouari R, Karaouzène T, Rendu J, Bidart M, Yassine S, Pierre V, Delaroche J, Hennebicq S, *et al.* Mutations in DNAH1, which encodes an inner arm heavy chain dynein, lead to male infertility from multiple morphological abnormalities of the sperm flagella. *Am J Hum Genet* 2014;**94**:95–104.

Coutton C, Escoffier J, Martinez G, Arnoult C, Ray PF. Teratozoospermia: spotlight on the main genetic actors in the human. *Hum Reprod Update* 2015;**21**:455–485.

Coutton C, Martinez G, Kherraf Z-E, Amiri-Yekta A, Boguenet M, Saut A, He X, Zhang F, Cristou-Kent M, Escoffier J, *et al.* Bi-allelic Mutations in ARMC2 Lead to Severe Astheno-Teratozoospermia Due to Sperm Flagellum Malformations in Humans and Mice. *Am J Hum Genet* 2019;**104**:331–340.

Coutton C, Vargas AS, Amiri-Yekta A, Kherraf Z-E, Ben Mustapha SF, Le Tanno P, Wambergue-Legrand C, Karaouzène T, Martinez G, Crouzy S, *et al.* Mutations in

CFAP43 and CFAP44 cause male infertility and flagellum defects in Trypanosoma and human. *Nat Commun* 2018;**9**:686.

Dam TJP van, Kennedy J, Lee R van der, Vrieze E de, Wunderlich KA, Rix S, Dougherty GW, Lambacher NJ, Li C, Jensen VL, *et al.* CiliaCarta: An Integrated And Validated Compendium Of Ciliary Genes. *bioRxiv* 2017;123455.

Dong FN, Amiri-Yekta A, Martinez G, Saut A, Tek J, Stouvenel L, Lorès P, Karaouzène T, Thierry-Mieg N, Satre V, *et al.* Absence of CFAP69 Causes Male Infertility due to Multiple Morphological Abnormalities of the Flagella in Human and Mouse. *Am J Hum Genet* 2018;**102**:636–648.

Elam CA, Wirschell M, Yamamoto R, Fox LA, York K, Kamiya R, Dutcher SK, Sale WS. An axonemal PP2A B-subunit is required for PP2A localization and flagellar motility. *Cytoskelet Hoboken NJ* 2011;**68**:363–372.

Fu G, Wang Q, Phan N, Urbanska P, Joachimiak E, Lin J, Wloga D, Nicastro D. The I1 dynein-associated tether and tether head complex is a conserved regulator of ciliary motility. *Mol Biol Cell* 2018;**29**:1048–1059.

GTEx Consortium. Human genomics. The Genotype-Tissue Expression (GTEx) pilot analysis: multitissue gene regulation in humans. *Science* 2015;**348**:648–660.

Heuser T, Dymek EE, Lin J, Smith EF, Nicastro D. The CSC connects three major axonemal complexes involved in dynein regulation. *Mol Biol Cell* 2012;**23**:3143–3155.

Inaba K. Molecular basis of sperm flagellar axonemes: structural and evolutionary aspects. *Ann N Y Acad Sci* 2007;**1101**:506–526.

Kherraf Z-E, Amiri-Yekta A, Dacheux D, Karaouzène T, Coutton C, Christou-Kent M, Martinez G, Landrein N, Le Tanno P, Fourati Ben Mustapha S, *et al.* A Homozygous Ancestral SVA-Insertion-Mediated Deletion in WDR66 Induces Multiple

Morphological Abnormalities of the Sperm Flagellum and Male Infertility. *Am J Hum Genet* 2018;**103**:400-412

Krausz C, Riera-Escamilla A. Genetics of male infertility. *Nat Rev Urol* 2018;**15**:369–384.

Liu W, He X, Yang S, Zouari R, Wang J, Wu H, Kherraf Z-E, Liu C, Coutton C, Zhao R, *et al.* Bi-allelic Mutations in TTC21A Induce Asthenoteratospermia in Humans and Mice. *Am J Hum Genet* 2019;**104**:738–748.

Lorès P, Coutton C, El Khouri E, Stouvenel L, Givelet M, Thomas L, Rode B, Schmitt A, Louis B, Sakheli Z, *et al.* Homozygous missense mutation L673P in adenylate kinase 7 (AK7) leads to primary male infertility and multiple morphological anomalies of the flagella but not to primary ciliary dyskinesia. *Hum Mol Genet* 2018;**27**:1196–1211.

Martinez G, Kherraf Z-E, Zouari R, Fourati Ben Mustapha S, Saut A, Pernet-Gallay K, Bertrand A, Bidart M, Hograindleur JP, Amiri-Yekta A, *et al.* Whole-exome sequencing identifies mutations in FSIP2 as a recurrent cause of multiple morphological abnormalities of the sperm flagella. *Hum Reprod Oxf Engl* 2018;**33**:1973-1984

Mizuno K, Shiba K, Okai M, Takahashi Y, Shitaka Y, Oiwa K, Tanokura M, Inaba K. Calaxin drives sperm chemotaxis by Ca^{2+}-mediated direct modulation of a dynein motor. *Proc Natl Acad Sci U S A* 2012;**109**:20497–20502.

Ohta T, Essner R, Ryu J-H, Palazzo RE, Uetake Y, Kuriyama R. Characterization of Cep135, a novel coiled-coil centrosomal protein involved in microtubule organization in mammalian cells. *J Cell Biol* 2002;**156**:87–99.

Ray PF, Toure A, Metzler-Guillemain C, Mitchell MJ, Arnoult C, Coutton C. Genetic abnormalities leading to qualitative defects of sperm morphology or function. *Clin Genet* 2017;**91**:217–232.

Sapiro R, Tarantino LM, Velazquez F, Kiriakidou M, Hecht NB, Bucan M, Strauss JF. Sperm antigen 6 is the murine homologue of the Chlamydomonas reinhardtii central apparatus protein encoded by the PF16 locus. *Biol Reprod* 2000;**62**:511–518.

Satir P, Christensen ST. Structure and function of mammalian cilia. *Histochem Cell Biol* 2008;**129**:687–693.

Sha Y-W, Xu X, Mei L-B, Li P, Su Z-Y, He X-Q, Li L. A homozygous CEP135 mutation is associated with multiple morphological abnormalities of the sperm flagella (MMAF). *Gene* 2017a;**633**:48–53.

Sha Y-W, Xu X, Mei L-B, Li P, Su Z-Y, He X-Q, Li L. A homozygous CEP135 mutation is associated with multiple morphological abnormalities of the sperm flagella (MMAF). *Gene* 2017b;**633**:48–53.

Shamoto N, Narita K, Kubo T, Oda T, Takeda S. CFAP70 Is a Novel Axoneme-Binding Protein That Localizes at the Base of the Outer Dynein Arm and Regulates Ciliary Motility. *Cells* 2018;**7**(9).

Shen Y, Zhang F, Li F, Jiang X, Yang Y, Li X, Li W, Wang X, Cheng J, Liu M, *et al.* Loss-of-function mutations in QRICH2 cause male infertility with multiple morphological abnormalities of the sperm flagella. *Nat Commun* 2019;**10**:433.

Tang S, Wang X, Li W, Yang X, Li Z, Liu W, Li C, Zhu Z, Wang L, Wang J, *et al.* Biallelic Mutations in CFAP43 and CFAP44 Cause Male Infertility with Multiple Morphological Abnormalities of the Sperm Flagella. *Am J Hum Genet* 2017;**100**:854–864.

The UniProt Consortium. UniProt: the universal protein knowledgebase. *Nucleic Acids Res* 2017;**45**:D158–D169.

Urbanska P, Joachimiak E, Bazan R, Fu G, Poprzeczko M, Fabczak H, Nicastro D, Wloga D. Ciliary proteins Fap43 and Fap44 interact with each other and are essential for proper cilia and flagella beating. *Cell Mol Life Sci CMLS* 2018;**75**:4479–4493.

Urbanska P, Song K, Joachimiak E, Krzemien-Ojak L, Koprowski P, Hennessey T, Jerka-Dziadosz M, Fabczak H, Gaertig J, Nicastro D, *et al.* The CSC proteins FAP61 and FAP251 build the basal substructures of radial spoke 3 in cilia. *Mol Biol Cell* 2015;**26**:1463–1475.

Wambergue C, Zouari R, Fourati Ben Mustapha S, Martinez G, Devillard F, Hennebicq S, Satre V, Brouillet S, Halouani L, Marrakchi O, *et al.* Patients with multiple morphological abnormalities of the sperm flagella due to DNAH1 mutations have a good prognosis following intracytoplasmic sperm injection. *Hum Reprod Oxf Engl* 2016;**31**:1164–1172.

Wang Y, Yang J, Jia Y, Xiong C, Meng T, Guan H, Xia W, Ding M, Yuchi M. Variability in the morphologic assessment of human sperm: use of the strict criteria recommended by the World Health Organization in 2010. *Fertil Steril* 2014;**101**:945-949

Xu Y, Cao J, Huang S, Feng D, Zhang W, Zhu X, Yan X. Characterization of tetratricopeptide repeat-containing proteins critical for cilia formation and function. *PloS One* 2015;**10**:e0124378.

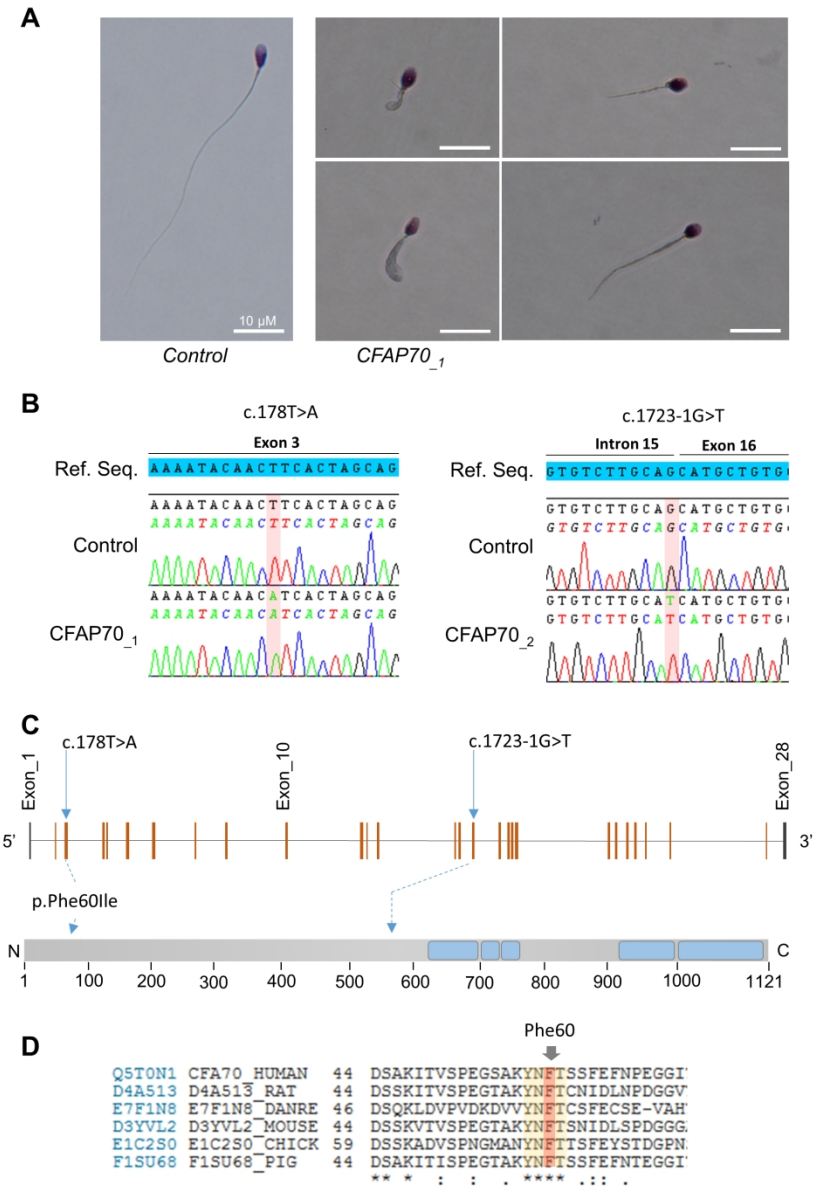
A
10 μM
Control
CFAP70_1
B
c.178T>A
Exon 3
Ref. Seq.
AAAATACAACTTCACTAGCAG
Control
CFAP70_1
c.1723-1G>T
Intron 15
Exon 16
Ref. Seq.
GTGTCTTGCAGCATGCTGTG
Control
CFAP70_2
C
Exon_1
c.178T>A
Exon_10
c.1723-1G>T
Exon_28
5'
3'
p.Phe60Ile
N
C
1
100
200
300
400
500
600
700
800
900
1000
1121
D
Phe60
Q5T0N1 CFA70_HUMAN 44 DSAKITVSPEGSAKYNFTSSFEFNPEGGI
D4A513 D4A513_RAT 44 DSSKITVSPEGTAKYNFTCNIDLNPDGGV
E7F1N8 E7F1N8_DANRE 46 DSQKLDVPVDKDVVYNFTCSFECSE-VAH
D3YVL2 D3YVL2_MOUSE 44 DSSKVTVSPEGTAKYNFTSNIDLSPDGGG
E1C2S0 E1C2S0_CHICK 59 DSSKADVSPNGMANYNFTTSFEYSTDGPN
F1SU68 F1SU68_PIG 44 DSAKITISPEGTAKYNFTSSFEFNTEGGI

Figure 1

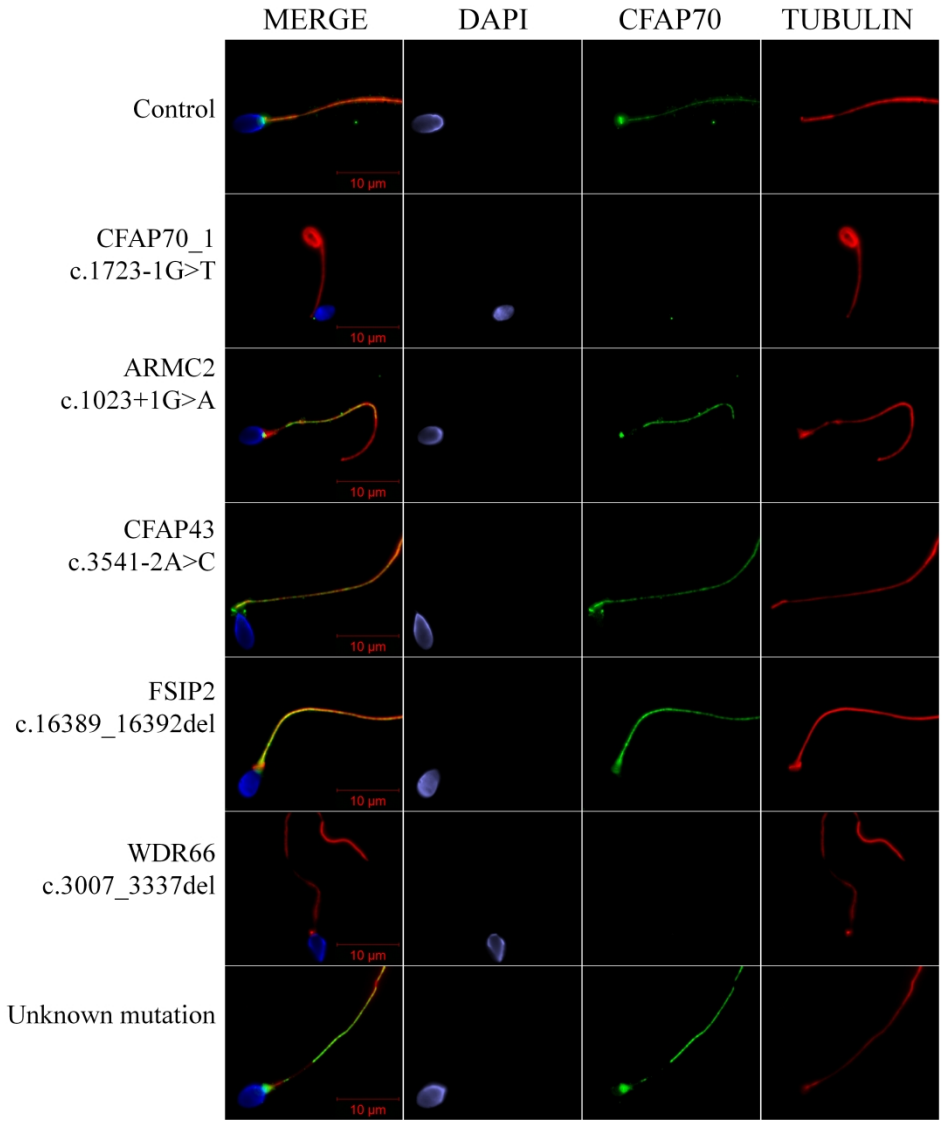

figure 2

1150x1300mm (96 x 96 DPI)

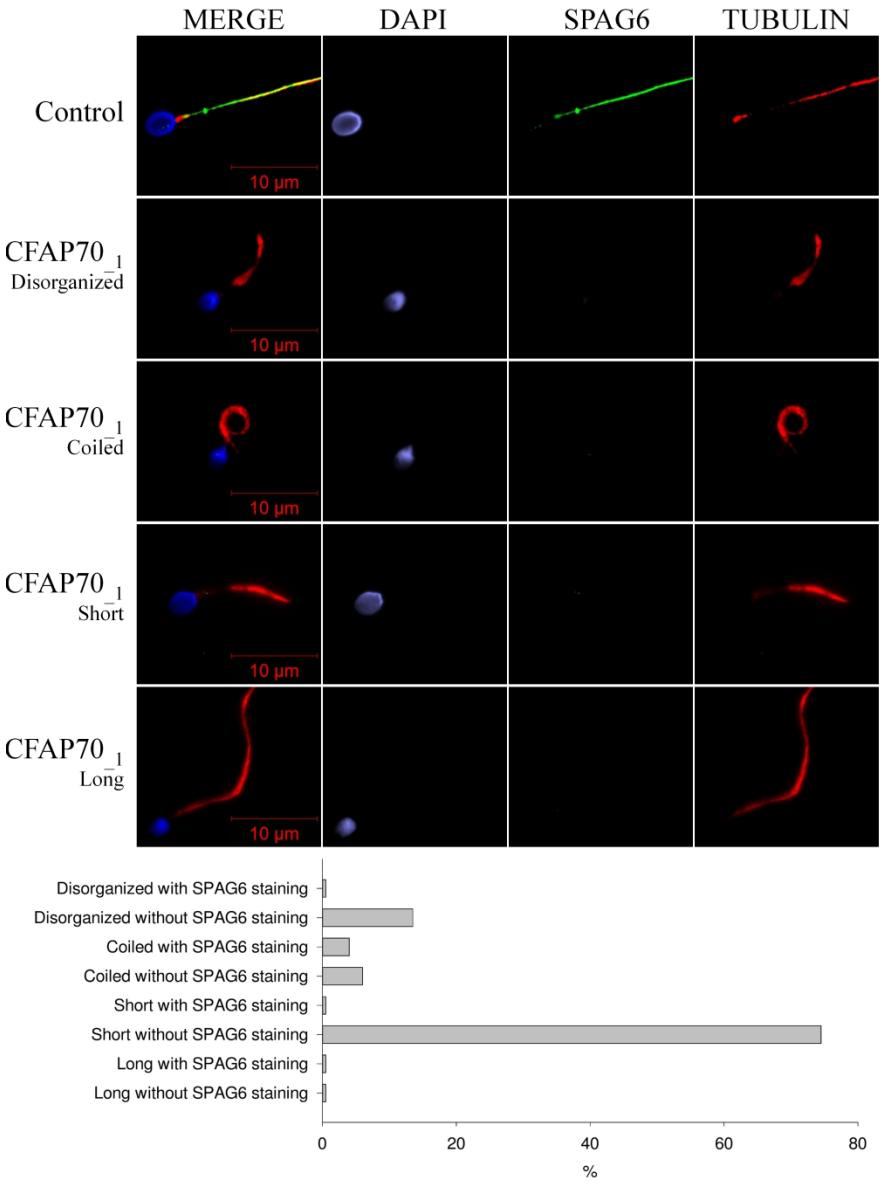

Figure 3

1076x1423mm (96 x 96 DPI)

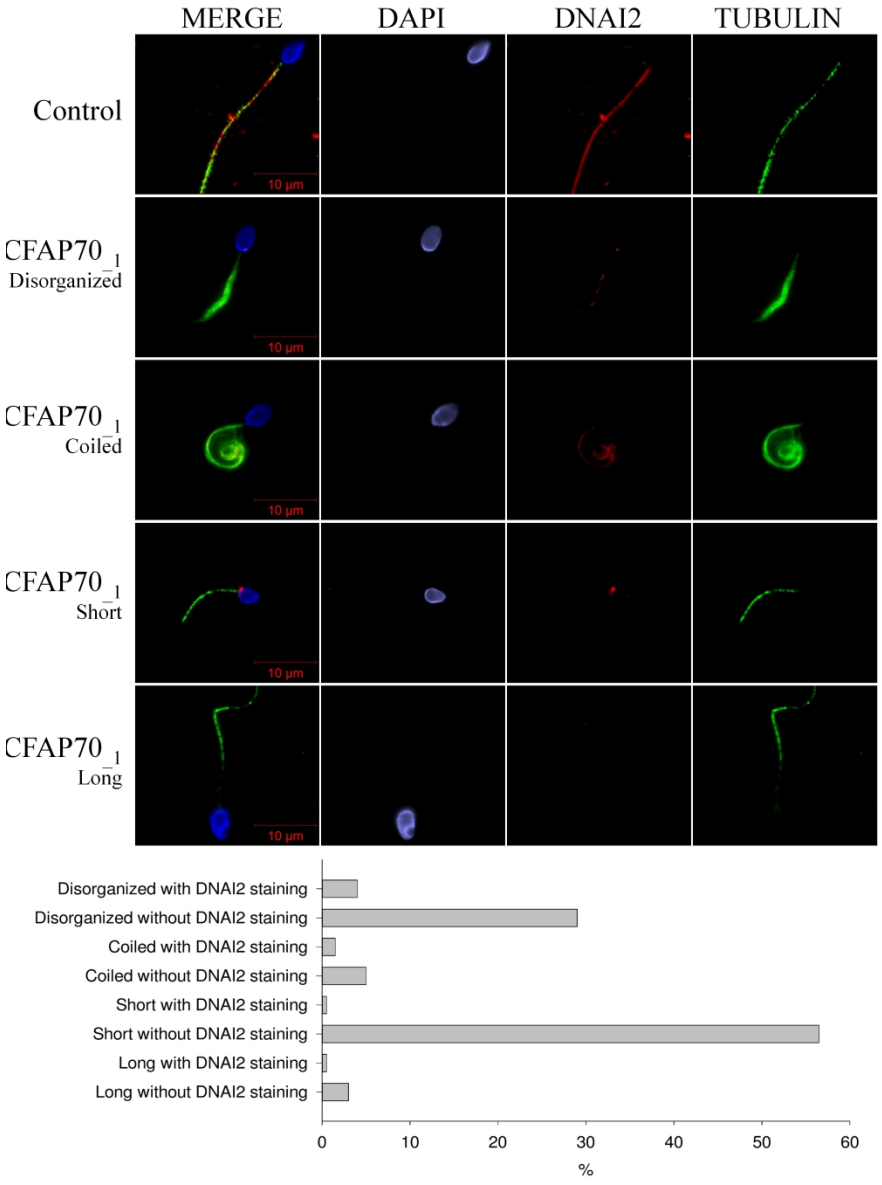

Figure 4

1076x1423mm (96 x 96 DPI)

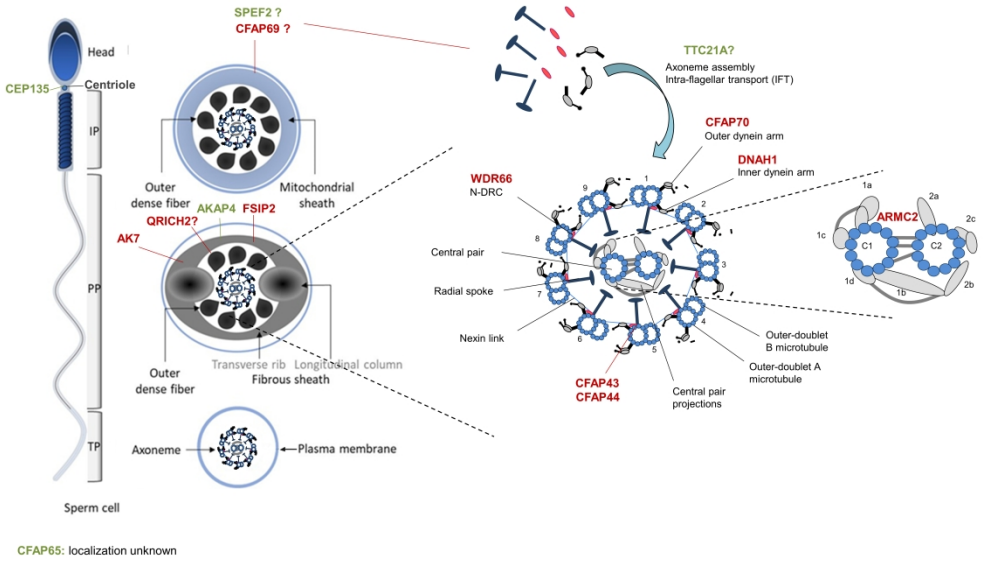
SPEF2 ?
CFAP69 ?
Head
CEP135
Centriole
IP
PP
TP
Outer dense fiber
Mitochondrial sheath
AKAP4
FSIP2
QRICH2?
AK7
Outer dense fiber
Transverse rib
Longitudinal column
Fibrous sheath
Axoneme
Plasma membrane
Sperm cell
TTC21A?
Axoneme assembly
Intra-flagellar transport (IFT)
CFAP70
Outer dynein arm
DNAH1
Inner dynein arm
WDR66
N-DRC
Central pair
Radial spoke
Nexin link
CFAP43
CFAP44
Central pair projections
Outer-doublet B microtubule
Outer-doublet A microtubule
ARMC2
C1
C2
CFAP65: localization unknown

Figure S1

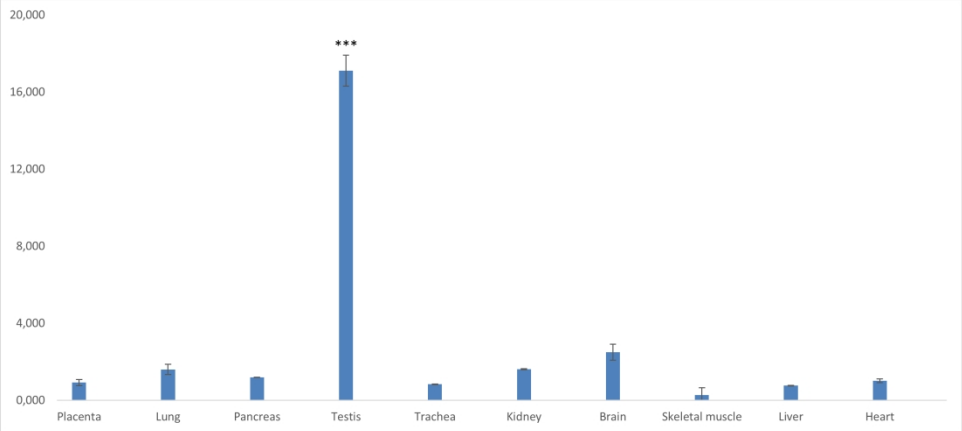
20,000
16,000
12,000
8,000
4,000
0,000
***
Placenta
Lung
Pancreas
Testis
Trachea
Kidney
Brain
Skeletal muscle
Liver
Heart

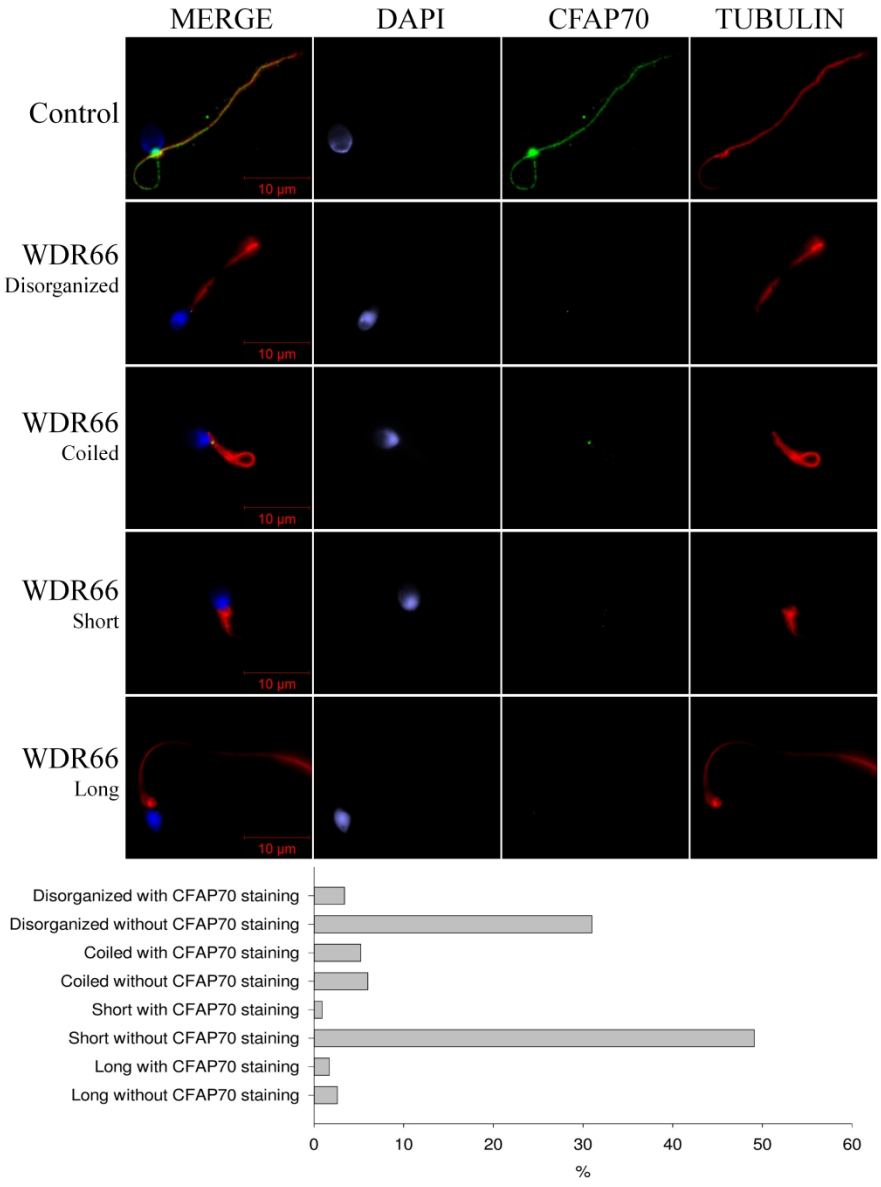

1098x1405mm (96 x 96 DPI)